Molecular Therapy
Nucleic Acids
Original Article

Block or degrade? Balancing on- and off-target effects of antisense strategies against transcripts with expanded triplet repeats in DM1

Najoua El Boujnouni,[1,4] M. Leontien van der Bent,[1,3,4] Marieke Willemse,[1] Peter A.C. 't Hoen,[1] Roland Brock,[1,2] and Derick G. Wansink[1]

[1]Department of Medical BioSciences, Research Institute for Medical Innovation, Radboud University Medical Center, 6525 GA Nijmegen, the Netherlands; [2]Department of Medical Biochemistry, College of Medicine and Medical Sciences, Arabian Gulf University, Manama 293, Bahrain

Antisense oligonucleotide (ASO) therapies for myotonic dystrophy type 1 (DM1) are based on elimination of transcripts containing an expanded repeat or inhibition of sequestration of RNA-binding proteins. This activity is achievable by both degradation of expanded transcripts and steric hindrance, although it is unknown which approach is superior. We compared blocking ASOs with RNase H-recruiting gapmers of equivalent chemistries. Two *DMPK* target sequences were selected: the triplet repeat and a unique sequence upstream thereof. We assessed ASO effects on transcript levels, ribonucleoprotein foci and disease-associated missplicing, and performed RNA sequencing to investigate on- and off-target effects. Both gapmers and the repeat blocker led to significant *DMPK* knockdown and a reduction in $(CUG)_{exp}$ foci. However, the repeat blocker was more effective in MBNL1 protein displacement and had superior efficiency in splicing correction at the tested dose of 100 nM. By comparison, on a transcriptome level, the blocking ASO had the fewest off-target effects. In particular, the off-target profile of the repeat gapmer asks for cautious consideration in further therapeutic development. Altogether, our study demonstrates the importance of evaluating both on-target and downstream effects of ASOs in a DM1 context, and provides guiding principles for safe and effective targeting of toxic transcripts.

INTRODUCTION

Antisense oligonucleotides (ASOs) are short, synthetic stretches of RNA or DNA analogs complementary to a target RNA. Various chemical modifications can increase the stability, affinity, and activity of these compounds.[1,2] ASOs can be broadly subdivided based on the mode of action. One class of ASOs, which we will refer to as blocking ASOs, functions through steric hindrance. These ASOs bind to their target sequence and thereby inhibit association of RNA-binding proteins, the splicing machinery, and/or ribosomes. The approved splice-switching oligonucleotides nusinersen (Spinraza) and eteplirsen (Exondys 51) are both blocking ASOs.[3] A second class of ASOs is the gapmers. These DNA-RNA chimeras contain a central "gap" consisting of DNA, flanked by "wings" that usually consist of chemically modified RNA nucleotides.[4,5] Gapmers recruit the cellular enzyme RNase H to degrade their target RNAs.

A group of disorders that is amenable to ASO therapy is repeat expansion disorders. Repeat expansions are known to cause over 50 different diseases, mainly neurodegenerative and neuromuscular in nature.[6] Several repeat expansion disorders are gain-of-function diseases caused by either (1) toxic RNAs, which sequester RNA-binding proteins, (2) toxic protein products, such as the polyglutamine protein produced in Huntington's disease (HD) and dipeptide-repeat-containing proteins in *C9orf72* amyotrophic lateral sclerosis (ALS)/frontotemporal dementia (FTD), or (3) a combination of both.[7] In many cases, blocking ASOs and gapmers can both be used to reduce the RNA or protein toxicity caused by the expanded repeat.

Myotonic dystrophy type 1 (DM1) is a prototypical RNA gain-of-function disorder caused by a large CTG repeat expansion in the 3′ UTR of the *DM1 Protein Kinase* (*DMPK*) gene. The expanded repeat in *DMPK* transcripts sequesters RNA-binding proteins such as muscleblind-like protein 1 (MBNL1), an important regulator of developmentally programmed RNA processing.[8] Several types of ASOs have been shown to be effective suppressors of expanded repeat activity in DM1, *in vitro* as well as in mouse models. On the one hand, we and others have described the use of blocking ASOs that target the CUG repeat using phosphorodiamidate morpholino, 2′-*O*-methyl phosphorothioate (2′-*O*-Me PS), and locked nucleic acids (LNAs)

Received 26 October 2022; accepted 13 April 2023;
https://doi.org/10.1016/j.omtn.2023.04.010.

[3]Present address: uniQure N.V., Paasheuvelweg 25a, 1105 BP Amsterdam, the Netherlands

[4]These authors contributed equally

Correspondence: Roland Brock, Department of Medical BioSciences, Research Institute for Medical Innovation, Radboud University Medical Center, 6525 GA Nijmegen, the Netherlands.
E-mail: roland.brock@radboudumc.nl
Correspondence: Derick G. Wansink, Department of Medical BioSciences, Research Institute for Medical Innovation, Radboud University Medical Center, 6525 GA Nijmegen, the Netherlands.
E-mail: rick.wansink@radboudumc.nl

Table 1. ASO sequences and chemical modifications

Name	Sequence	Theoretical T_m (°C)
Repeat blocking	**C*A*G*C*A*G*C*A*G*C*A*G*C*A*G**	68.0
Repeat gapmer	**C*A*G*C***A*G*C*A*G*C*A*G*C*A***G*C*A*G**	65.6
DMPK blocking	**G*A*G*C*G*G*U*U*G*U*G*A*A*C*U*G*G**	66.6
DMPK gapmer	**C*G*G*A*G***C*G*G*T*T*G*T*G*A*A***C*U*G*G*C**	64.9
Control blocking	**G*A*C*G*A*C*G*A*C*G*A*C*G*A*C**	63.7
Control gapmer	**G*A*C*G***A*C*G*A*C*G*A*C*G*A*C***G*A*C**	53.4

Bold underline, 2′-*O*-Me; non-bold non-underline, DNA; *, phosphorothioate linkage.

chemistries.[9–13] These ASOs function primarily by displacing MBNL1 from the expanded repeat. On the other hand, gapmers have been employed to target the expanded CUG repeat,[11,14] as well as other parts of the transcript,[15–17] to induce degradation of *DMPK* RNA. In these cases, 2′-*O*-(2-methoxyethyl) (MOE), constrained ethyl (cEt), 2′-*O*-Me, and LNA modifications of the flanking regions were explored.

Overall, for the targeting of repeat expansion RNAs, there are four different possibilities, namely targeting of either the repeat or a non-repeat sequence by either a blocking or gapmer ASO. With respect to sequence, targeting of sequences up- or downstream of the repeat should yield a higher specificity for *DMPK* transcripts than targeting of the repeat itself, a sequence motif that is also present in at least 75 other transcripts.[18] However, use of repeat-specific ASOs allows for preferential targeting of CUG-expanded *DMPK* transcripts over normal *DMPK* transcripts. Gapmers only need to bind once to induce cleavage of an RNA and function through a catalytic mode of action, while steric hindrance at the repeat likely requires many more ASO molecules per transcript, as it depends on shielding a sufficiently large proportion of the repeat from protein binding. Thus, gapmers might show activity at lower concentrations.

To our knowledge, an in-depth comparison of blocking and gapmer ASOs with similar chemical modifications and for two different target sequences has not been performed yet. Targeting of the *DMPK* transcript offers an ideal test case for this purpose as distinct readouts exist at the level of the RNA target itself and for subsequent events downstream. We compared pairs of fully 2′-*O*-Me-modified blocking and partly 2′-*O*-Me-modified gapmer PS ASOs targeted against the CUG repeat or a region upstream of the repeat. Both target sequences had been independently shown to be active in previous studies, albeit with MOE- instead of 2′-*O*-Me-modified nucleosides in the case of the *DMPK* gapmer.[9,11,15] ASOs were delivered in a human skeletal muscle cell model for DM1 using the cell-penetrating peptide PepFect14,[19] which we have previously shown to be an efficient delivery vehicle in myoblasts.[20] We studied the effect of the ASOs on target RNA levels, as well as on the level of two hallmarks of DM1: nuclear expanded CUG-containing ribonucleoprotein (RNP) foci and DM1-associated missplicing.[21] Furthermore, by performing RNA sequencing (RNA-seq) for cells after ASO treatment, we assessed both on- and off-target effects of the ASOs on a transcriptome-wide level.

RESULTS

The repeat-blocking ASO and both gapmers lead to downregulation of *DMPK* RNA

In this study, we compared four different ASOs—blocking vs. gapmer for CUG repeat vs. non-repeat targeting sequences—to investigate the balance between on- and off-target effects in DM1. We used fully 2′-*O*-Me-modified blocking and partly 2′-*O*-Me-modified gapmer ASOs targeted against the CUG repeat and against a region upstream of the repeat (Table 1). In all cases, the entire backbone contained phosphorothioate linkages. Of these four ASOs, the non-repeat-targeting blocking ASO was expected to be the only ASO without a therapeutic effect, as it neither targets a region involved in the sequestration of MBNL1 nor causes degradation of the transcript. We tested the ASOs in immortalized myoblasts derived from a congenital DM1 patient with a short repeat of 13 CTG triplets and an expanded repeat of approximately 2,600 triplets in *DMPK*. The long repeat offers many binding sites for the CAG ASOs, whereas the short repeat offers only maximally two binding sites per *DMPK* transcript. The unique, non-repeat *DMPK* target sequence is present once in both transcript variants. This target sequence has been successfully used before, albeit with an MOE- instead of a 2′-O-Me-modified ASO. The myoblasts used in this study are a suitable cell model for DM1, as they exhibit a number of disease-specific features, including expression of expanded *DMPK* transcripts, presence of $(CUG)_{exp}$ RNA foci and DM1-associated missplicing of various transcripts.[22–25]

An overview of the experimental setup and a schematic representation of the *DMPK* transcript with the various target sites is shown in Figures 1A and 1B. Myoblasts were transfected with polyplexes consisting of the cell-penetrating peptide PepFect14 and ASOs. As control ASOs, a $(GAC)_5$ blocking ASO and $(GAC)_6$ gapmer were used, as described previously.[10,12] Cells treated with only peptide PepFect14 and untreated cells were included as additional controls. After 24 h, cells were washed, fresh proliferation medium was added, and cells were cultured for another 24 h. At this point, cells were either harvested for RNA isolation to assess gene expression and alternative splicing (Table 2) or fixed for microscopy to visualize *DMPK* transcripts.

To assess ASO efficacy, we first stained *DMPK* transcripts by RNA FISH, using a fluorescently labeled $(CAG)_6C$ probe and a set of 48 fluorescent probes spaced along the body of the *DMPK* transcript (Figure 1B). The $(CAG)_6C$ probe only detects RNAs from the expanded *DMPK* allele because a sufficient number of probes needs to bind for a detectable fluorescence signal. We will refer to these foci as "$(CUG)_{exp}$ foci." The probe set against the body of the

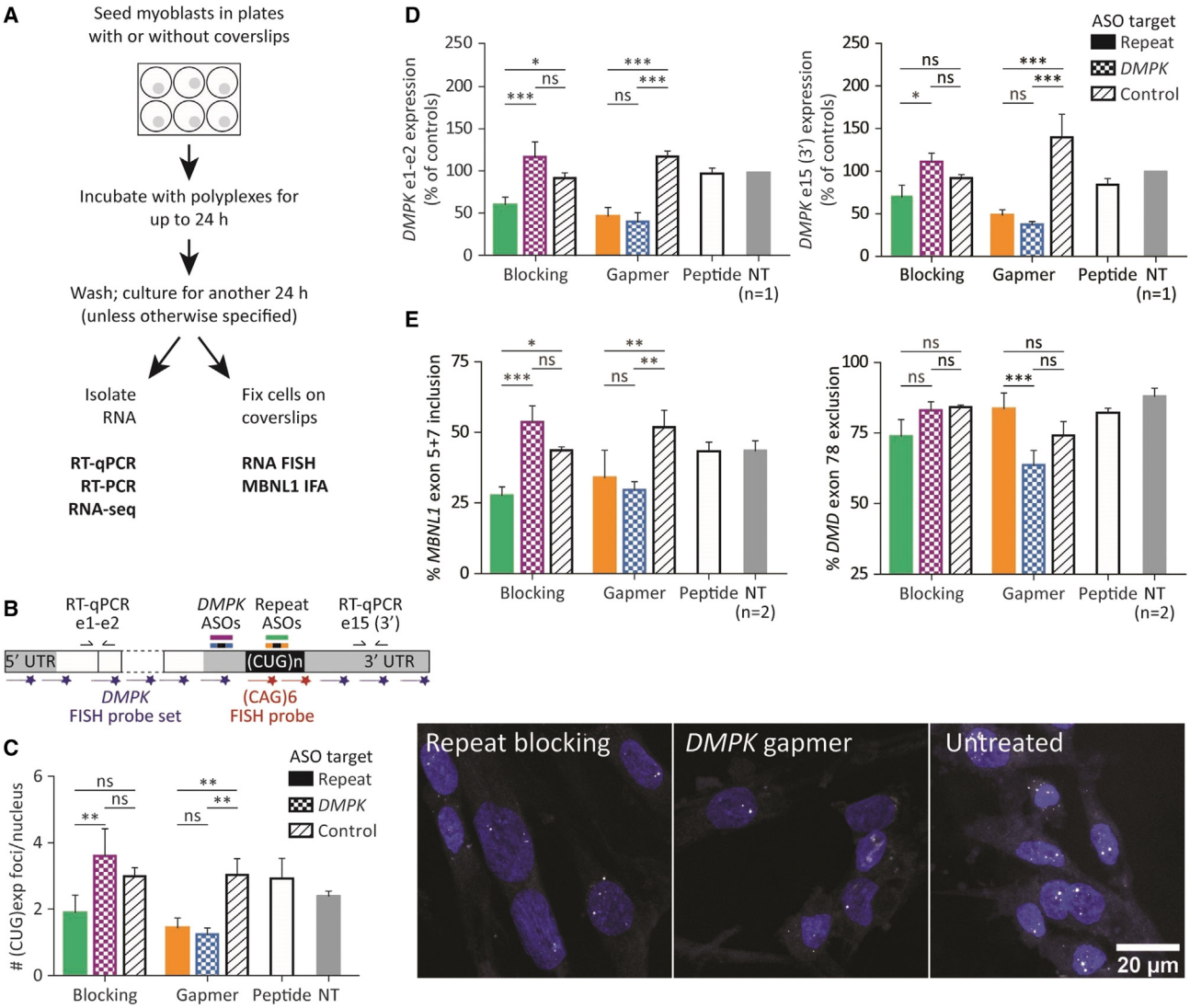

Figure 1. Both gapmers and the repeat blocking ASOs led to *DMPK* knockdown and reduced the number of repeat RNA foci

(A) Schematic overview of the experimental setup. (B) Schematic overview of the *DMPK* transcript (not to scale), with relative positions of ASO target sites, qRT-PCR primer binding sites and FISH probe binding sites. (C) Number of nuclear $(CUG)_{exp}$ foci as determined by RNA FISH and representative images of the RNA FISH after incubation of DM11 cells with polyplexes containing 100 nM of the indicated ASOs. Signal of the TYE-563-labeled $(CAG)_6C$ probe is shown in grays, DAPI was used as nuclear counterstain and is shown in blue. NT, untreated. (D) *DMPK* expression after incubation with polyplexes containing 100 nM of the indicated ASOs, as determined by qRT-PCR for amplicons *DMPK* e1-e2 and *DMPK* e15 (3′). Bar graphs show the mean ± SEM of three independent experiments, unless otherwise stated. A two-way ANOVA was used to compare the effect of each ASO to its respective type. Significance values shown in the graphs were calculated using Bonferroni post hoc tests between rows (target sequence). *p < 0.05, ***p < 0.001. (E) Alternative splicing of *MBNL1* exons 5 and 7 and *DMD* exon 78 for DM11 myoblasts treated with polyplexes at an ASO concentration of 100 nM (with roughly 15%–20% inclusion of *MBNL1* exon 5 + 7 and 60% *DMD* exon 78 exclusion in CRISPR-Cas9-corrected myoblasts as reference). Each bar indicates the mean ± SEM of three independent experiments, unless otherwise stated. A two-way ANOVA was used to compare the effect of each ASO with its respective type. Significance values shown in the graphs were calculated using Bonferroni post hoc tests between rows (target sequence). *p < 0.05, **p < 0.01, ***p < 0.001. See Figure S4 for representative primary RT-PCR data.

transcript, on the other hand, detects both short and expanded *DMPK* alleles. Based on previous findings by our group for DM1[26] and others for repeat transcripts in *C9orf72* ALS/FTD,[27] we assume that each focus represents one transcript, and we will therefore refer to the FISH foci detected with the *DMPK* probe set as "*DMPK* transcripts." We know that foci detection by the $(CAG)_6C$ LNA FISH probe is not significantly compromised by pretreatment with the repeat blocker (Figure S1). In addition, competitive inhibition of binding of the FISH probe by the repeat blocker may be anticipated; however, cells are permeabilized and washed extensively prior to *in situ* hybridization, thereby removing essentially all of the non-bound repeat blocker before the fluorescent LNA probe is added.

Table 2. Overview of PCR primers used in this study

Target	Forward primer (5′ → 3′)	Reverse primer (5′ → 3′)
DMPK e1-e2	ACTGGCCCAGGACAAGTACG	CCTCCTTAAGCCTCACCACG
DMPK e15 (3′)	TGCCTGCTTACTCGGGAAATT	GAGCAGCGCAAGTGAGGAG
GAPDH	CCCGCTTCGCTCTCTGCTCC	CCTTCCCCATGGTGTCTGAGCG
HPRT1	TGACACTGGCAAAACAATGCA	GGTCCTTTTCACCAGCAAGCT
MBNL1 e4-e8	GGCTGCCCAATACCAGGTCA	CTTGTGGCTAGTCAGATGTTCGG
DMD e77-e79	TTAGAGGAGGTGATGGAGCA	GATACTAAGGACTCCATCGC

The repeat blocker and both gapmers led to a significant reduction of nuclear $(CUG)_{exp}$ foci (Figure 1C; $p < 0.01$). Compared with the repeat blocker, the gapmers tended toward a slightly larger reduction of the total number of *DMPK* transcripts, which suggests that also transcripts with a short repeat were downregulated (Figure S2; average of 1.3 and 2.1 foci/nucleus with the *DMPK* and repeat gapmer, respectively, vs. an average of 2.8 foci/nucleus with the repeat blocker). We note that the *DMPK* probe set introduced a much larger degree of interexperimental variation than observed for the repeat probe, which can be explained by the higher background signal for the *DMPK* probe set in combination with automated foci counting. Moreover, the hybridization efficiency of the probe set and therefore the signal intensity depends on the dynamic ensemble of structural conformations of the *DMPK* transcripts in the nucleus.

We then measured *DMPK* expression using qRT-PCR for two amplicons on opposite ends of the transcript, one spanning the junction from exon 1 to exon 2, and one downstream of the $(CUG)_n$ repeat (Figure 1B), as described previously.[11] In line with the RNA FISH results, we found that both the repeat and the *DMPK* gapmer led to a clear and significant knockdown of total *DMPK* by more than 50% (Figure 1D). It has been shown before that mRNAs from both alleles are present in approximately equal quantities, and thus a reduction of more than 50% is indicative of knockdown of both the short and the expanded allele,[26] which is anticipated for gapmers that are active upon a single binding event. The repeat blocker also reduced *DMPK* expression, which was not unexpected as this type of ASO has been shown before to use an unknown, RNase H-independent pathway for target gene knockdown.[9–11] The *DMPK*-blocking and control gapmer ASOs slightly, although non-significantly, upregulated *DMPK* expression.

ASO-mediated *DMPK* knockdown is not predictive of the extent of splicing correction

Degradation of *DMPK* transcripts as well as blockage of repeats should liberate the splice factor MBNL1 and thus affect splicing as a subsequent (downstream) effect. We assessed alternative splicing of two well-known, misspliced transcripts in DM1: *MBNL1* and *DMD*. In DM1, aberrant splicing leads to increased inclusion of exons 5 and 7 in *MBNL1*, and to exclusion of exon 78 in *DMD*.[28,29] Consistent with the downregulation of *DMPK* expression and the decrease in the number of nuclear $(CUG)_{exp}$ foci, both gapmers led to a reduction of *MBNL1* exon 5 and 7 inclusion in DM1 myoblasts as expected for correction of the DM1 phenotype (Figures 1E and S3). Although the repeat blocking ASO showed considerable, but milder, *DMPK* reduction than the gapmers, at 100 nM of ASO the effect of the repeat blocker on *MBNL1* splice correction was comparable with that of the *DMPK* gapmer, which is in line with a liberation of MBNL1 in the absence of prominent degradation of the transcript. Interestingly, the repeat gapmer showed a reduced activity. By comparison, there was no correction of *DMD* exon 78 exclusion for all ASOs under the tested conditions as only a slight although non-significant reduction was detected for the repeat blocker and the *DMPK* gapmer (Figure 1E). Thus, with respect to splicing the repeat gapmer showed a reduced activity, and the *DMPK* gapmer and repeat blocker showed a splice site-dependent activity.

Overall, we note that there was a strong positive correlation in DM11 cells for the readouts that directly addressed the presence of *DMPK* transcripts, namely qRT-PCR and FISH, whereas the degree of correlation with downstream splicing was variable and differed per splice site, with *MBNL1* splicing showing a better correlation than *DMD* splicing (Figure S4). Overall, the repeat blocker performed better in the restoration of splice patterns than would be expected based on the degree of *DMPK* knockdown. From these data, we conclude that *DMPK* knockdown per se is not a straightforward predictor of downstream splice correction.

The repeat blocker outperforms the gapmers in dispersing MBNL1 from repeat RNA foci

The reduction of *DMPK* transcripts only partially correlated with splice correction in our DM1 cell model. Sequestration of MBNL proteins by the expanded repeat is thought to lead to the majority of the missplicing events in DM1.[30–32] By binding to the expanded CUG repeat, the repeat blocker supposedly leads to MBNL release directly, whereas the gapmers likely lead to MBNL dispersal as a consequence of RNase H-mediated degradation of *DMPK* RNA. We were therefore interested to learn whether both types of ASOs differ in their efficiency of MBNL release. To test this idea, we treated DM11 myoblasts with ASOs for various times up to 24 h, after which they were fixed and MBNL1 was visualized by immunofluorescence. As in the previous experiments, a time point at 48 h was also included, in which cells were washed after 24 h and then cultured for 24 h without ASOs.

MBNL1 immunofluorescence showed that the number of nuclear MBNL1 foci was reduced by all of the three ASOs that also reduced *DMPK* expression and nuclear $(CUG)_{exp}$ foci (Figure 2A;

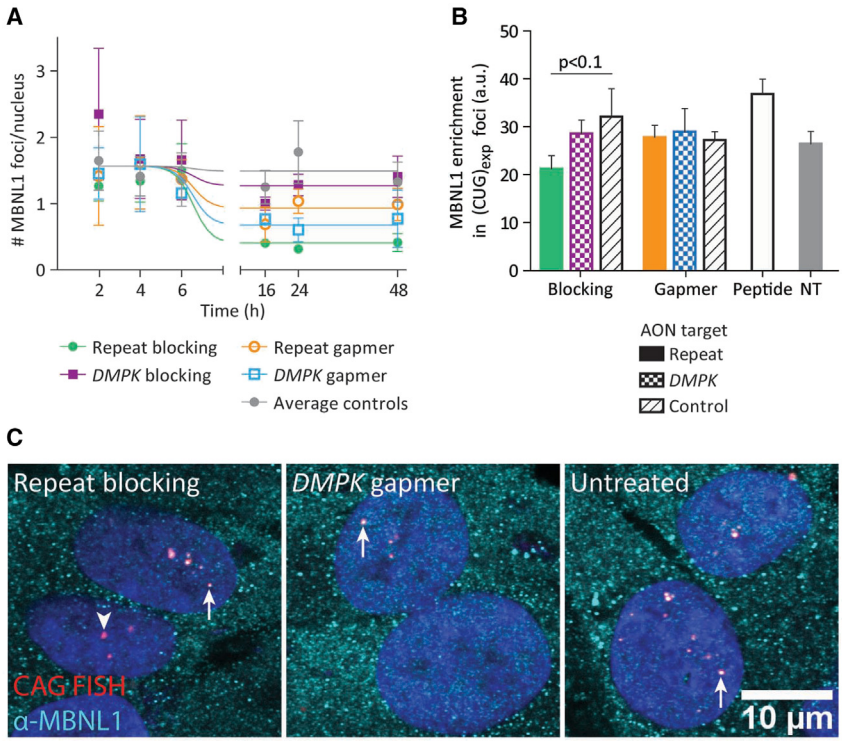

Figure 2. Effect of ASO treatment on MBNL1 sequestration by CUG repeat RNA

(A) The number of MBNL1 foci in DM11 cells in relation to the incubation time with ASOs, as detected by immunofluorescence. Each point indicates the mean ± SEM of two to four independent experiments. A dose-response (sigmoidal) curve fit was performed to analyze the relation between the number of MBNL1 foci throughout time (as a measure of the dynamics of ASO efficacy), for which the top value was constrained to be equal for each dataset. Model comparisons using the extra sum of squares F test indicated that the bottom values of the curves differed between the datasets ($p = 0.0549$). (B) MBNL1 enrichment in $(CUG)_{exp}$ foci, as detected by RNA FISH combined with immunofluorescent detection of MBNL1. Shown is the mean increase of the MBNL1 signal in $(CUG)_{exp}$ foci compared with the mean nuclear MBNL1 intensity. Each bar indicates the mean ± SEM of three independent experiments. (C) Representative overlay images of RNA FISH with the $(CAG)_6C$ probe (red) combined with the MBNL1 IFA (cyan) and the nuclear counterstain (DAPI) in blue. Complete overlap of the red and cyan shows as white (examples indicated by arrows), while lower MBNL1 signal results in predominantly red foci (example indicated by the arrowhead).

$p = 0.055$). Although not significantly different between groups, this trend in reduction appeared to be most pronounced for the repeat blocker (best-fit value for "bottom" parameter 0.41 (95% CI, −0.20–1.0) compared with 0.68 (95% CI, 0.14–1.2) for the repeat gapmer and 0.93 (95% CI, 0.37–1.49) for the *DMPK* gapmer). After 16 h, all conditions had reached a steady state and the repeat-targeting gapmer that had shown hardly any effect in splice correction was also the least effective in MBNL1 displacement. There was no indication for a difference in kinetics.

To further investigate the effect of the various ASOs on MBNL1 sequestration by the expanded repeat, we combined immunofluorescence staining of MBNL1 with RNA FISH against the expanded CUG repeat after 48 h. The repeat blocker and both gapmers led to a reduction of the total number of MBNL1 foci; however, only the repeat blocking ASO led to a noticeable reduction of MBNL1 signal in the $(CUG)_{exp}$ foci (Figures 2B and 2C; $p < 0.1$). While these data demonstrate a direct visualization of the activity of the repeat blocker, this again shows a lack of a one-to-one correlation of on-target and downstream events, i.e., *DMPK* RNA knockdown, MBNL1 protein release, and missplicing correction.

RNA-seq reveals activation of the interferon response by all ASOs and additional off-target effects on gene expression by the repeat gapmer

After having assessed ASO activities on the level of the direct molecular target and with respect to splicing of two downstream events, we aimed to obtain a comprehensive understanding of the effects of the tested ASOs on a transcriptome-wide level, with the discrimination of targeting of the CUG sequence in *DMPK* (and resulting effects) as on-target and targeting of other transcripts—including those containing a short CUG sequence—as off-target effects. For this purpose, we performed RNA-seq on poly(A)-enriched samples. We included immortalized myoblasts derived from an unaffected individual (C25) as a reference for a healthy situation. As the *DMPK* blocking ASO had not shown any beneficial effects in the previous experiments, we did not include this condition for RNA-seq. On average, 77 ± 4 million clean reads were obtained per sample, with an average total mapping ratio of 81% ± 2.5% and a unique mapping ratio of 70% ± 2.3%.

Gene expression data of a total of 21,410 genes were generated. Pearson correlation and hierarchical clustering analysis of the gene expression profiles showed that the C25 cells were clearly distinguishable from the DM11 cells, both treated and untreated (Figure S5). To our surprise, both control ASOs led to differential regulation, especially upregulation, of quite a large number of genes (Table 3). Compared with the control blocking ASO, the effect of the control gapmer on gene expression was more than 2-fold larger. There was, however, considerable overlap between the two ASOs: 89% of the genes that were differentially expressed in response to the control blocking ASO were also affected by the control gapmer (Figure S6). We performed PANTHER overrepresentation tests for Reactome pathways, and found that genes involved in interferon signaling were specifically upregulated in response to treatment of DM11 myoblasts with the control ASOs (Table S1; Figure S6). For the control

Table 3. Summary of gene expression changes of control ASOs vs. untreated DM11 myoblasts

	Control blocking	Control gapmer
Upregulated	551	1397
Downregulated	49	132

Number of genes that were significantly up- or downregulated compared with untreated control DM11 myoblasts ($|\log_2\text{-fold change}| \geq 1$ and probability ≥ 0.8). Two independent replicates were included per condition.

gapmer, genes involved in interleukin signaling were also enriched. Overall, interferon signaling appeared to be similarly induced by all ASOs, while interleukin signaling was more prominent for the repeat gapmer and control gapmer (Figure 3A). To increase the power of our analyses and to correct for these non-specific effects, we pooled the three controls: control blocking ASO, control gapmer and untreated DM11 cells.

While the repeat blocker and *DMPK* gapmer had only minor effects on overall gene expression, the repeat gapmer led to both up- and downregulation of almost 1,500 genes (6.8% of the 21,410 genes with measurable expression) compared with the control group ($|\log_2\text{-fold change}| \geq 1$ and probability ≥ 0.8; Tables 4 and S2). Notably, many of these genes were found to be differentially expressed only in response to the repeat gapmer, and not to the control gapmer. PANTHER overrepresentation tests of these uniquely differentially expressed genes showed that most of the gene expression changes induced by the repeat gapmer were related to the cell cycle (Figure 3B; Table S1).

To cross-validate the transcriptome-wide sequencing data with our qRT-PCR analyses, we first confirmed that both gapmers led to significant downregulation of *DMPK* of up to 82% (Figure 3C; Table S3). Again, this indicates that the gapmers targeted both short and expanded repeat-containing RNAs. The repeat blocker led to a minor, non-significant reduction of *DMPK* levels of approximately 25%, which is also in line with our previous observations. Remarkably, the repeat gapmer additionally led to significant changes in the expression of the genes immediately adjacent to *DMPK* in the DM1 locus, upregulating *SIX5* by a factor of 2 and downregulating *DMWD* by a factor of 2.8 compared with controls. We speculate that this deregulation may be secondary to the differential regulation of transcription factors known to bind to the promoters of these genes, such as *MYOD1*, which was downregulated by the repeat gapmer, and *STAT5A*, which was upregulated (Table S2).

Next, we investigated expression of the splicing factors that are most prominently implicated in the spliceopathy in DM1: *MBNL1*, *MBNL2*, and *CELF1*. Next to autoregulation of *MBNL1* splicing and expression, *MBNL1* mRNA levels are also regulated by *CELF1*.[34,35] *CELF1* expression was not altered by any of the three ASOs, but *MBNL1* expression was markedly reduced by the repeat gapmer, whereas *MBNL2* levels were increased by this ASO (2.3- and 2.6-fold, respectively).

As the repeat-targeting ASOs have the potential to also target other CUG repeat-containing transcripts, we investigated the levels of a number of transcripts other than *DMPK* that contain CUG repeat tracts. From this analysis, it emerged that, out of 48 genes that were expressed, the repeat blocker only led to significant downregulation of one gene, *OTUD4* (Figure 3D; Table S3). The repeat gapmer, on the other hand, led to downregulation of many other CUG repeat-containing transcripts: 28 of the 48 genes were knocked down by more than 50%. The degree of knockdown affected by the repeat-targeting gapmer only showed a weak linear correlation with repeat length ($R^2 = 0.15$). Two transcripts that contain an intronic CUG repeat and that are linked to various types of corneal dystrophy, *ZEB1* and *TCF4*,[36–38] and four transcripts that contain a CAG repeat were not significantly affected by either of the repeat-targeting ASOs ($|\log_2\text{-fold change}| < 1$), indicating that the effect is specific for exonic CUG repeats.

The repeat-blocking ASO most efficiently corrects DM1-associated alternative splicing

Finally, we analyzed our RNA-seq data for effects on alternative splicing induced by the ASOs. We first confirmed splice correction of *MBNL1* exon 5 by the repeat blocker and *DMPK* gapmer and of *DMD* exon 78 by the repeat blocker ($p < 0.05$; Table S4). To assess all DM1-associated splicing changes, we compiled a reference list of DM1-associated splicing events from several papers that investigated transcriptome-wide splicing changes,[39–41] as well as from an RNA-seq dataset generated by our group, where we compared the same DM11 myoblasts that we used here with isogenic controls in which the repeat region was excised using CRISPR-Cas9 genome editing.[22] These edited myoblasts do not show any evidence of gross chromatin remodeling or changes in the expression of the three genes upstream and downstream of *DMPK*.[42] Also, we know that the hypermethylation in the locus, associated with congenital DM1, is still present after repeat excision in the myoblasts.[43] From the comparison with the isogenic controls (Table S4), only 17% of the DM1-specific splice modes used in this study were uniquely derived.

Overall, we found that, compared with the control group, the two repeat-targeting ASOs caused more significantly altered splicing events with a false discovery rate ≤ 0.05 than the *DMPK* gapmer (Figure 4A). The repeat blocker changed 131 events and the repeat gapmer 130 events. By comparison, the *DMPK* gapmer only led to 60 significantly altered splicing events. These differences are in line with our qRT-PCR analysis of splice events. Intriguingly, the number of DM1-associated events, such as *NCOR2* e45 and *TPM2* e6, was vastly different between the ASOs: 6% for the repeat gapmer, 10% for the *DMPK* gapmer, but 27% for the repeat blocker. Not only was the number of known DM1-associated splicing changes largest in the cells treated with the repeat blocker, but the effect size was generally also larger than that of the two gapmers. We further zoomed in on the known DM1-associated genes and found that there was considerable overlap between the splicing events that were changed by ASO treatment; in this case, however, especially between the repeat blocker and the *DMPK* gapmer (Figure 4B). The effect was generally larger and more significant for the repeat blocker than for the *DMPK*

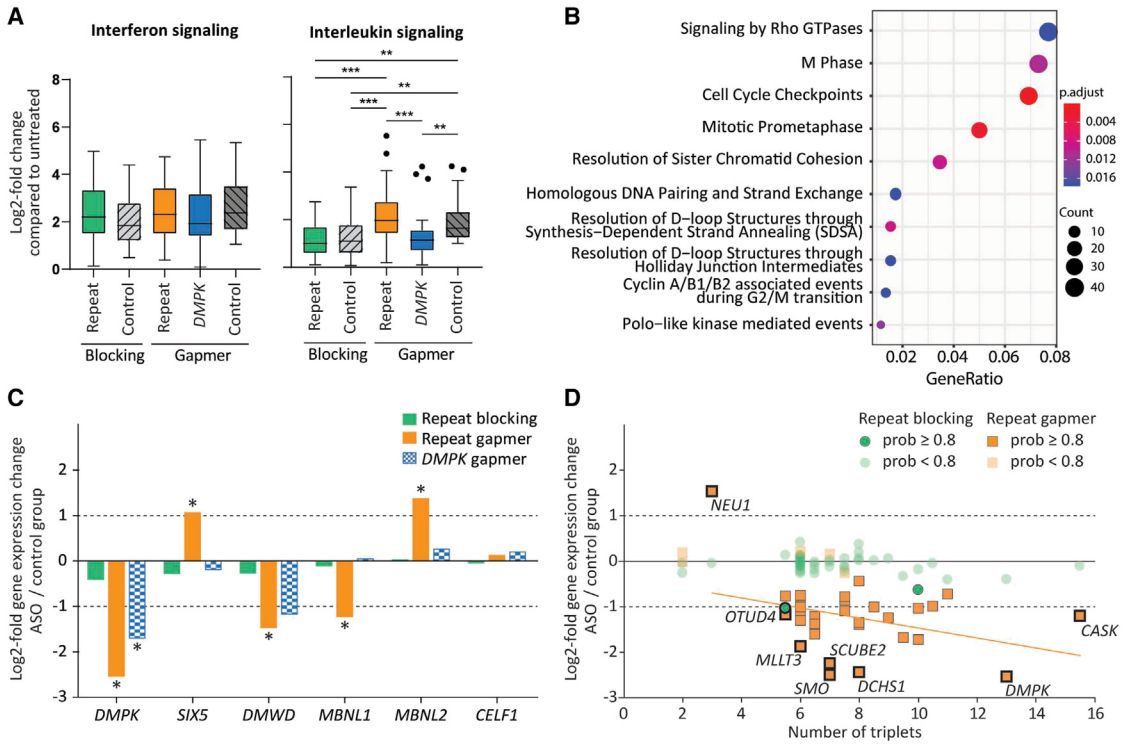

Figure 3. Effects of ASO treatment on gene expression in DM11 myoblasts

(A) Effect of ASO treatment on genes involved in interferon and interleukin signaling. All genes that were differentially regulated by the control gapmer compared with untreated were included. Boxplots were drawn using Tukey's method and show median and 25th to 75th percentiles; whiskers show minimal and maximum values, or 1.5 times the interquartile range, in which case values exceeding this cutoff are indicated with black circles. Medians were compared using a Kruskal-Wallis test by ranks followed by Dunn's multiple comparison tests. **$p < 0.01$, ***$p < 0.001$. (B) Reactome pathway enrichment analysis of genes that were differentially regulated by the repeat gapmer.[33] The top 10 enriched pathways (adjusted $p < 0.05$) are shown. (C) Gene expression changes of genes in the *DMPK* locus and various DM1-associated splicing factors compared with the control group. *Significantly altered gene expression (log_2-fold change > 1 and probability ≥0.8). (D) Effect of repeat-targeting ASOs on $(CUG)_n$-containing transcripts. The log_2-fold change compared with the control group is plotted against the number of CUG triplets, taking the average if the two alleles differed in repeat length. When multiple repeats were present in one gene, the longest repeat tract was used. Only transcripts with a mean FPKM of the control group ≥1 and for which the number of triplet repeats could be derived from the RNA-seq data are shown. Different shades indicate the probability score of the expression difference. Gene names of some extreme examples are indicated (see also Table S3).

gapmer; and, of the top 10 DM1-associated alternative splice events, six were the same between the two ASOs (Figure 4C). This indicates that, although the extent may differ, correction of splicing by these ASOs is mediated through a similar pathway, which most likely is due to release of *MBNL* proteins.

To determine whether the observed splicing changes were a correction of DM1-associated missplicing, we compared the ASO-treated cells with unaffected control cells. For events altered by the repeat gapmer, there was very little overlap with the other ASOs or the healthy control (Figure 4C; Table S4). The repeat gapmer occasionally even induced splicing changes in the opposite direction compared with the other ASOs or to the unaffected controls, which suggests that some DM1-associated missplicing events might be aggravated by this ASO. Notably, in agreement with this observation we had also observed a slight but consistent increase in DMD exon 78 exclusion. Importantly, the repeat blocker and *DMPK* gapmer almost exclusively induced splicing changes toward the splicing pattern observed in C25-unaffected control cells, confirming our previous results that these ASOs decrease DM1-associated spliceopathy (Figure 4D; Table S4).

DISCUSSION

Antisense therapies have emerged as a promising new treatment option for various heritable neuromuscular and neurodegenerative disorders.[44,45] For some disorders, the mode of action of the ASO is dictated by the type of mutation. In Duchenne muscular dystrophy, for instance, the aim of antisense treatment is skipping of an exon that contains a premature stop codon or interrupts the open reading frame, and thus steric blocking ASOs must be used.[46] By comparison, for a number of neuromuscular and neurodegenerative disorders that are caused by microsatellite repeat expansions, both blocking ASOs and RNase H-recruiting gapmers show promise. For example, in DM1, both ASO types can ultimately reduce MBNL sequestration.[8,47] Increased understanding of the consequences, advantageous and

Table 4. Summary of gene expression changes of repeat- and *DMPK*-targeting ASOs in DM11 myoblasts

	Repeat blocking	Repeat gapmer	*DMPK* gapmer
Upregulated	0/0	527/726	19/57
Downregulated	2/2	590/732	7/26

Number of genes that were significantly up- or downregulated compared with the control group ($|\log_2\text{-fold change}| \geq 1$ and probability ≥ 0.8). Some of the genes overlapped with those found for the control ASOs, implying that these gene expression changes were non-specific (see Table S2). The number of non-overlapping changes out of the total number of changes is shown. Three independent replicates were included for each of the three ASOs. The control group consisted of untreated, control blocking- and control gapmer-treated cells, with two independent replicates per control condition.

disadvantageous, inherent to both ASO strategies is required to direct the development of effective and safe ASO therapies. Therefore, we performed a direct comparison of 2′-*O*-Me PS ASOs against different target sequences (repeat vs. non-repeat) and using different modes of action (steric blocking vs. RNase H recruitment).

We used a set of ASOs with the same phosphorothioate (PS) and 2′-*O*-methyl (2′-*O*-Me) modifications to be able to make a direct comparison of target sequence and mode-of-action *in vitro*. We acknowledge that these observations, without further confirmation, only hold true for the tested chemical modifications and target sequences and are not generalizable to all ASOs with other chemical modalities, target sequences, and/or mechanisms. Particularly with the ever-growing possibilities in ASO chemistries, it is important to realize that a different type of chemistry might have a different activity profile. Nevertheless, our results clearly point out the need for in-depth characterization of on-target and downstream effects, thus we consider the impact of our results of general importance. Moreover, as we aimed to compare different ASO types, we chose to pool the three controls rather than comparing each ASO to its respective control. Pooling of the three controls might have generated a larger variation (in comparison to separate controls) and introduced a certain bias toward larger changes, potentially excluding cumulative effects caused by, for example, several smaller changes exerted by a specific ASO. However, the lack of consensus on the ideal ASO control (untreated, non-targeting, scrambled) convinced us to include all three controls in our study and analysis. Furthermore, our approach increases the statistical power so that the most important effects of functional ASOs can better be demonstrated. This ultimately leads to fewer false positive results caused by the sequence or chemistry of any of the control ASOs.

Based on the mode of action, all ASOs showed activity on the target transcript. Our 15-mer repeat blocking ASO led to downregulation of *DMPK* in DM1 myoblasts, although the degree of knockdown was more modest than in previous studies, in which we mainly used myoblasts derived from the DM500 transgenic mouse model and a longer ASO.[9,11] DM500 cells contain only the expanded human *DMPK* allele, and therefore the maximum allele-specific knockdown is 100%, as opposed to the maximum of 50% in the human patient-derived myoblasts that we used here. Knockdown of the target transcript achieved by the two gapmers was substantial and this effect can be attributed to both the direct function that gapmers exert on their target transcript and their requirement of a single binding instance to do this. In line with the degree of *DMPK* knockdown, nuclear $(CUG)_{exp}$ foci were reduced by all three ASOs. The repeat blocker was in fact as efficient in correcting downstream alternative splicing events that are typical for DM1 as the *DMPK* gapmer ASO, whereas the repeat gapmer showed limited effectiveness. On the level of MBNL1 foci, the repeat blocker more efficiently displaced MBNL1 from $(CUG)_{exp}$ foci than the gapmer oligonucleotides. Thus, very clearly, there is no strong correlation of on-target and downstream events. Even for *MBNL1* mis-splicing which is a direct target of MBNL1, the efficiency differed per ASO in a way that did not correlate with *DMPK* downregulation.

The number of detected $(CUG)_{exp}$ and MBNL1 foci can deviate due to the sensitivity of myoblast cultures to confluency and differentiation. In addition to this, experiment-specific conditions (e.g., magnification, thresholding,and noise settings) can cause weak MBNL1 foci to be missed during automated image analysis. In RNA FISH the nucleoplasmic background is generally lower, hence weaker $(CUG)_n$ foci are detected and counted than when using an antibody against MBNL1 which also detects free nucleoplasmic MBNL1 proteins. It is also important to realize that the quantitative detection of *DMPK* transcripts *in situ* cannot be directly translated to their quantification in RT-PCR. The greater variation *in situ* using microscopy techniques is likely caused by the high flexibility in RNA folding during RNA processing and transit through the nucleus, resulting in many semi-stable conformations, and in the differential, spatiotemporal binding of RNA proteins. As a consequence, expanded *DMPK* transcripts, as RNP particles, may bind variable amounts of MBNL1 protein, presumably affecting foci size. This in turn may shield the repeat sequence to a variable degree from binding to the fluorescent probes, generating foci with different intensities.

The *DMPK* blocking ASO was not expected to influence *DMPK* expression or downstream splicing, as it neither induces RNase H1-mediated degradation, nor is expected to displace MBNL1 proteins from the repeat. Instead, this ASO appeared to cause a slight upregulation of the number of $(CUG)_{exp}$ foci and *DMPK* transcript levels, which, however, did not reach significance. It is intriguing that the *DMPK* blocking ASO thus may have the opposite effect of the repeat blocker. It was recently found that some blocking-type ASOs induce no-go decay, which is induced by stalling of the ribosomal machinery.[48] Similar to nonsense-mediated decay, this process depends on translation. Although both ASOs target sequences that are located in the 3′ UTR and thus are by definition not translated, it has been suggested that the expanded CUG repeat is subject to repeat-associated non-ATG (RAN) translation.[49,50] This might explain why the repeat blocker ASO induced knockdown of the expanded repeat alleles, whereas the *DMPK* blocking ASO did not. A trend toward upregulation of *DMPK* was also observed for the control gapmer ASO. Why these ASOs showed this behavior requires further investigation.

At a fixed concentration of 100 nM for all ASOs, despite the different working mechanisms, we found that the extent of on-target effect

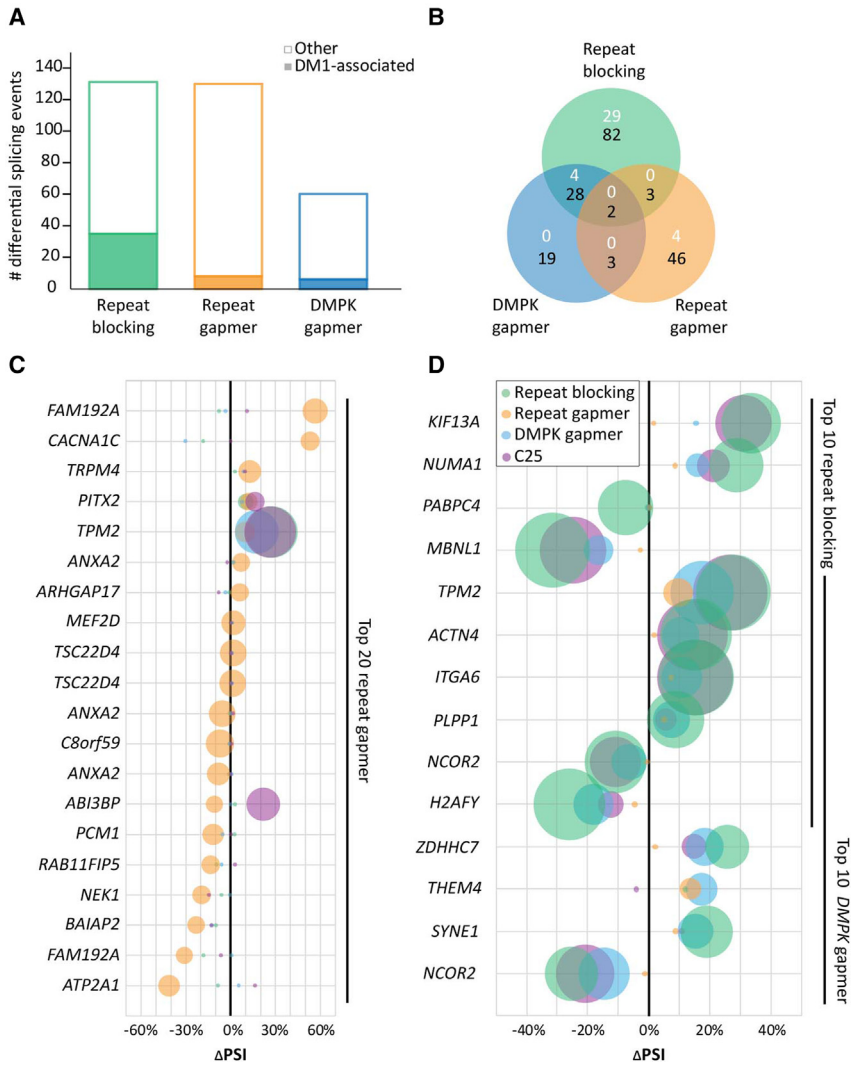

Figure 4. Effects of ASO treatment on alternative splicing

(A) Number of significantly changed alternative splicing events (false discovery rate [FDR] ≤ 0.05) compared with the control group. Bottom (filled): splicing events in genes that were previously found to be misspliced in DM1; top (outline only): splicing events in other genes. (B) Venn diagram of altered DM1-associated splicing events in ASO-treated cells compared with the control group (in white FDR < 0.05, in black $p < 0.05$). (C) Top 20 altered DM1-associated splicing events in cells treated with the repeat gapmer. (D) Top 10 altered DM1-associated splicing events in cells treated with the repeat blocker and the *DMPK* gapmer. Gene names are indicated for each row, and the changes in percentage spliced in (ΔPSI (ASO, controls) or (C25, untreated)) are plotted on the x axis. Circle sizes are inversely proportional to the p value (i.e., a higher degree of significance correspond to larger circles). For (B), (C), and (D), only events with at least five counts on average in any of the groups were included in the analyses (see also Table S4).

(*DMPK* knockdown) was not fundamentally different between the ASOs, yet, at the level of splice correction, striking differences in potency were observed. We also did not observe any cell toxicity effect by either the peptide or the ASO at the tested dose. This, albeit for one given ASO concentration, allowed us to study and compare the impact of the working mechanisms and on-target and downstream effects exerted by the ASOs that results in a strong effect. Additional studies are required to understand ASO-specific dose-effect correlations at other oligonucleotide concentrations.

DM11 cells serve as the standard for *in vitro* assessment of ASO efficacy and are extensively used in the field of DM1. Although use of other DM1-affected cell lines would be ideal, the availability thereof is limited and, for this study, these considerably different cell lines would likely introduce a high level of variability, taking away from the nuanced changes that can be detected upon ASO treatment.

The appropriate choice of a control cell line is an important question to assess the impact of ASOs in particular for more downstream activities as these should be more dependent on the genetic background. In our case, we used a control from an unaffected healthy individual. One may argue that an isogenic control with the repeat removed through gene editing may be the more appropriate control.[22] However, at the time of study, this cell line was not fully characterized yet. Moreover, in our study most experiments concern the comparison of affected cells with/without ASO and comparison with unaffected cells is of less importance.

All tested ASOs led to induction of genes relating to interferon signaling. Whether this activity translates into a toxic effect *in vivo* is difficult to predict. In line with previous reports, we observed that genes involved in interferon signaling were already more highly expressed in untreated DM1 cells than in unaffected control cells.[51,52] It could therefore be envisaged that DM1 cells are more sensitive to induction of the interferon response. As only some of the ASOs contained CpG motifs, we surmise that this response was largely independent of CpG recognition. Interferon signaling in response to non-CpG oligonucleotides has been reported previously, and has been ascribed to cellular nucleic acid sensing receptors such as toll-like receptor 3 (TLR3), TLR7, TLR9, PKR, RAGE, and MDA5.[53–57] At this point, we also cannot exclude that the observed immune response was induced by the cell-penetrating peptide, although a study on an earlier PepFect variant revealed that the induction of an inflammatory response was negligible.[58] Nonetheless, this potential concern should be revisited for PepFect14.

In this study, we investigated missplicing as a downstream effect of ASOs, based on a toxic RNA gain-of-function model. Other disease mechanisms, such as RAN translation, RNA interference (RNAi), and *DMPK*/*SIX5* haploinsufficiency have also been described for DM1.[59] With respect to the best mode of action, RNase H-mediated degradation is expected to more effectively inhibit RAN translation and repeat-mediated RNAi. On the other hand, haploinsufficiency would be aggravated by this approach, as healthy transcripts also appeared to be degraded by the gapmers. Downstream, blocking ASOs are proving to be efficacious in several *in vitro* as well as *in vivo* studies and, with their favorable safety profile, are now reaching clinical trials.[60] The fact that the relative contribution of each of these different disease mechanisms to the complex manifestation of DM1 is still enigmatic makes it difficult to weigh these considerations at this point in time.

We clearly found that the repeat gapmer led to downregulation of not only *DMPK*, but a number of other CUG repeat-containing transcripts as well, which may not be unexpected as the target sequence of this oligonucleotide is indeed not unique to *DMPK*. This observation also coincides with our previous finding that a $(CAG)_7$ gapmer showed reduced repeat-length selectivity compared with blocking ASOs.[11] As only transcript levels of *DMPK* and other CUG repeat-containing mRNAs were assessed in that study, it was not yet known whether this ASO caused downstream splice correction. To our surprise, the repeat gapmer did not mediate efficient correction of splicing events, and in some cases even aggravated DM1-associated missplicing. Based on these data, we conclude that targeting the *DMPK* CUG repeat using a CAG repeat gapmer may not be a feasible therapeutic option for DM1.

A disconnect between knockdown efficiency and downstream splice correction has been observed by others as well.[10,14] Moreover, in many early-stage studies, especially screenings for the most efficient target sequence for RNase H-mediated degradation, only knockdown of the target transcript was evaluated. Here, however, we provide evidence that *DMPK* knockdown per se may not be a solid predictor for downstream splicing correction and that ASO profiling and selection need to comprise profiling of off-target effects on a broader scale.

By conducting a broader analysis, we here showed that the repeat blocking ASO $(CAG)_5$, even though being seemingly less effective in knocking down *DMPK* transcripts, was able to correct downstream splicing defects caused by expanded CUG repeat RNA even more consistently than the gapmers. With limited unwanted effects as well, out of the set of tested oligonucleotides, this ASO is thus expected to be more safe for use and suitable for further pre-clinical development. Using DM1 as an exemplary case of an RNA-mediated and ASO-treatable disorder, we thus show that profound analysis of ASO-associated effects is needed to determine their therapeutic potential. Investigating the balance between on- and off-target ASO activities already at the *in vitro* stage, will likely accelerate further pre-clinical and clinical development for antisense-based therapeutics.

MATERIALS AND METHODS

Cell-penetrating peptide and ASOs

The amphipathic peptide PepFect14, a stearylated cell-penetrating peptide with the sequence stearyl-AGYLLGKLLOOLAAAALOOLL-NH_2 where O is ornithine and -NH_2 is a C-terminal amidation[19] was purchased from PepScan (Lelystad, the Netherlands). ASOs were synthesized and purified by HPLC followed by a Na^+ salt exchange at Integrated DNA Technologies (IDT, Leuven, Belgium). All ASOs contained 2′-*O*-methyl and phosphorothioate modifications. All gapmers had a gap of 10 nucleotides and the length of the ASOs was adjusted such that the blocking and gapmer versions targeting the same sequence had comparable theoretical melting temperatures (T_m) (based on eu.idtdna.com/calc/analyzer, target-type RNA, standard settings, accessed June 1, 2022). The sequences and modifications of the ASOs, as well as the theoretical T_m values, are shown in Table 1.

Cell culture

Immortalized human DM1 myoblasts with an uninterrupted expanded repeat (DM11 cl5, $(CTG)_{13/2600}$) were derived from primary myoblasts from a DM1 patient. Immortalized human myoblasts from an unaffected individual were used (C25, $(CTG)_{5/14}$) as a control. Both cell lines were kindly provided by Dr. D. Furling and Dr. V. Mouly and described previously.[22,24] Myoblasts were grown in a 1:1 mix of Skeletal Muscle Cell Growth Medium (PromoCell, Heidelberg, Germany) with 1× GlutaMAX (Gibco; Thermo Fisher Scientific, Landsmeer, the Netherlands) and Ham's F-10 Nutrient Mix with GlutaMAX (Gibco), supplemented with 20% (v/v) HyClone Bovine Growth Serum Supplemented Calf (GE Healthcare, South Logan, UT). All tissue culture vessels were coated with 0.1% gelatin (Sigma G2500) in Milli-Q for at least 30 min prior to cell seeding. Cells were incubated at 37°C in humidified incubators with 7.5% CO_2. Cells were routinely tested for mycoplasm infections.

Polyplex formation and incubation

Nanoparticles consisting of ASOs and the cell-penetrating peptide PepFect14 (polyplexes) were formed at a charge (N/P) ratio of 3. This corresponds to a molar ratio of peptide:ASO of 9:1. Peptides and ASOs were diluted to 20× the final concentration, after which they were mixed by simultaneous pipetting against the wall of a PCR tube with the pipette tips in close contact. Polyplexes were then allowed to stabilize at room temperature for approximately 1 h.

For incubation with cells, polyplexes or peptides were pre-diluted to 2× the final concentration in serum-free Ham's F-10 Nutrient Mix. Medium on cells was replaced with half the final volume of Skeletal Muscle Cell Growth Medium supplemented with 1× GlutaMAX and 20% (v/v) HyClone Bovine Growth Serum Supplemented Calf. To this, an equal volume of pre-diluted polyplexes or peptides in serum-free Ham's F-10 Nutrient Mix was added. The final concentration of ASOs was 100 nM. After 24 h incubation, cells were washed once with PBS, after which fresh proliferation medium was added. To study the kinetics of ASO action, cells were incubated for 2, 4, 6, 16, or 24 h, followed by immediate fixation for microscopy.

RNA isolation and RT-PCR

Cells were seeded 1 day prior to the start of the experiment at a density of 100,000 cells per well in 6-well plates. RNA was isolated from 6-well plates at 48 h after the start of incubation with polyplexes using the Aurum total RNA mini kit (Bio-Rad, Veenendaal, the Netherlands) according to the manufacturer's instructions, including DNase treatment. As an additional step to ensure shearing of genomic DNA, lysates were pulled through a 0.5 mm syringe 15 times prior to the addition of ethanol. In general, 500 ng RNA (or the maximum volume of 15 μL in the case of low RNA yield) was used for cDNA synthesis using the iScript cDNA synthesis kit (Bio-Rad), which contains a mix of random hexamer and oligo(dT) primers, according to the manufacturer's instructions.

To assess *DMPK* expression, qRT-PCR was performed for two amplicons on either end of the *DMPK* transcript, one spanning the junction from exon 1 to exon 2 and one located 3′ from the CUG repeat in *DMPK* exon 15 (see Table 2 and Figure 1B). *GAPDH* and *HPRT1* were used as reference genes. Three microliters of 10-fold diluted cDNA sample were mixed in a final volume of 10 μL containing 5 μL of iQ SYBR Green Supermix (Bio-Rad) and 0.4 μM of each primer using the CAS-1200 automated pipetting system (QIAGEN, Venlo, the Netherlands). No template control (NTC) and no reverse transcriptase control (NRT) were included in each qRT-PCR run to detect possible contaminations. Samples were analyzed using a CFX96 Real-time System (Bio-Rad) using a two-step amplification protocol. A melting curve was obtained for each sample to confirm single product amplification.

To assess alternative splicing, PCRs were performed using Q5 High-Fidelity DNA Polymerase (New England BioLabs, Leiden, the Netherlands). The primers are listed in Table 2. For *DMD* an annealing temperature of 66°C was used, for *MBNL1* an annealing temperature of 69°C. PCR mixes consisted of 1× Q5 reaction buffer, 0.2 mM dNTPs (Invitrogen), 0.5 μM of forward and reverse primer each, 0.4 U Q5 High-Fidelity DNA polymerase and 2 μL 10× diluted cDNA in a total volume of 20 μL. The following program was run on the T100 Thermal Cycler (Bio-Rad): 3' 98°C, 35× (10″ 98°C, 20″ 66/69°C, 20″ 72°C), 10′ 72°C, ∞ 4°C. PCR products were analyzed on the QIAxcel Advanced capillary electrophoresis system (QIAGEN) using the DNA High Resolution Kit, along with the 15–600 bp alignment marker and 25–500 bp size marker. Again, NTC and NRT were included in each PCR run to detect possible contaminations. The amplicon of interest (*MBNL1* exon 5 and exon 7 inclusion, DMD exon 78 exclusion) was normalized to all other splice variant amplicons in each sample.

RNA FISH and immunofluorescence assays

One day prior to the start of the experiment, cells were seeded at a density of 100,000–150,000 cells per well in 6-well plates (containing 10 mm coverslips) or 15,000–25,000 cells per well in 48-well plates. At 48 h after start of incubation with the polyplexes, or at various time points during the experiment, cells on 10 mm coverslips in 6-well plates were fixed using 2% paraformaldehyde (PFA) in 0.1 M phosphate buffer. Cells were washed three times with ice-cold ethanol and stored at 4°C under ethanol until further handling. For RNA FISH only, the protocol as specified by Stellaris (LGC Biosearch Technologies, Petaluma, CA) was followed. In brief, cells were washed using Stellaris Wash Buffer A, then incubated overnight at 37°C with 10 ng/mL TYE-563 labeled $(CAG)_6C$ LNA probe and 125 nM of the Quasar-670 labeled *DMPK* probe set consisting of 48 different 18- to 20-nucleotide DNA probes spaced along the transcript (Stellaris). Both probes were diluted in hybridization buffer. Cells were then washed and nuclei were counterstained using 1 μg/mL DAPI in wash buffer. Images were acquired using a Zeiss LSM880 Laser Scanning Confocal Microscope (Zeiss, Oberkochen, Germany), using a 63× 1.4 NA oil immersion objective. Frame sequential z stacks were obtained in which fluorescence was excited at 405 nm (DAPI), 514 nm (TYE-563), and 633 nm (Quasar-670) and emission light collected between 410 and 585 nm (DAPI), 538–680 (TYE-563), and 638–754 nm (Quasar-670).

For RNA FISH followed by immunofluorescence assay (IFA) for MBNL1, PFA-fixed cells were washed three times with PBS, then washed once with ice-cold 70% ethanol and stored at 4°C under 70% ethanol until further handling. Cells were washed twice with PBS, then pre-hybridized for 20 min in 40% deionized formamide in 2× SSC buffer at room temperature. Finally, cells were incubated overnight at 37°C with 10 ng/mL TYE-563-labeled $(CAG)_6C$ LNA probe in hybridization mix consisting of 40% deionized formamide, 2× SSC, 2 mg/mL BSA, 100 mg/mL dextran sulfate, 0.1% Triton X-100, 1 mg/mL herring sperm DNA, 100 μg/mL yeast tRNA, and 2 mM VRC.

Prior to MBNL1 IFA, PFA-fixed cells were post-fixed using a 1:1 mixture of ice-cold acetone and methanol, then washed three times with PBS, and blocked for 1 h using a blocking buffer consisting of 0.1% Triton X-100 (v/v) (Sigma), 0.1% glycine (Merck) and 3% bovine serum albumin (Sigma A9647) in PBS. After this, cells were incubated overnight at 4°C with 1:10 diluted MB1a (4A8) monoclonal antibody against MBNL1 (Developmental Studies Hybridoma Bank) in blocking buffer without Triton X-100. After washing three times with PBS, cells were incubated for 1 h with secondary goat-anti-mouse Alexa Fluor 488-labeled antibody (2 μg/mL; Invitrogen) and DAPI (1 μg/mL; Sigma-Aldrich). When only MBNL1 was stained, cells were also incubated with primary polyclonal rabbit-anti-actin (1:100 diluted, A5060 Sigma) and secondary goat-anti-rabbit Alexa Fluor 568-labeled antibody (2 μg/mL; Invitrogen) to visualize the whole cell. Finally, cells were washed three times with PBS, dehydrated in ethanol and mounted on objective slides using Mowiol.

MBNL1 IFA-only samples were imaged on a Leica DMI6000B automated high-content microscope using a 63× 0.9 NA dry objective (Leica Microsystems, Wetzlar, Germany). Frame sequential images were obtained with an 89000 ET Sedat Quad filter set (Chroma, Bellows Falls, VT) with excitation filters 402/15 nm (DAPI), 490/20 nm (Alexa Fluor 488), 555/25 nm (TYE-563), and 645/30 nm (Cy5), and emission filters 455/50 nm (DAPI), 525/36 nm (AF488), 605/52 (TYE-563), and 705/72 nm (Cy5).

The combined MBNL1 IFA and RNA FISH samples were imaged on the Zeiss LSM880 confocal microscope using a 63× 1.4 NA oil immersion objective. Frame sequential images in a single confocal plane of 3.5 μm were obtained in which fluorescence was excited at 405 nm (DAPI), 488 nm (Alexa Fluor 488), and 561 nm (TYE-563), and emission light collected between 410 and 508 nm (DAPI), 493 and 558 nm (AF488), and 566 and 681 (TYE-563).

RNA-seq

For RNA-seq, replicates from two to three independent experiments were prepared. As described above, 100,000 cells were seeded per well of a 6-well plate. DM11 cells were treated for 24 h at a final ASO concentration of 100 nM. After 24 h, cells were washed once with PBS, then cultured for a further 24 h in proliferation medium. Untreated DM11 and C25 cells were also included as controls. RNA was isolated using the Aurum total RNA mini kit as described above. RNA concentration and quality were assessed using the QIAxcel RNA QC Kit (QIAGEN). Total RNA from two independent replicates of each of the negative controls (control blocking, control gapmer, and untreated ASOs), and three replicates of each of the tested ASO treatments (repeat blocking, repeat gapmer and *DMPK* gapmer) and the unaffected controls (C25) were submitted to BGI Genomics (Hong Kong) for RNA-seq. Library preparation was done on poly(A)-enriched samples and libraries were sequenced paired-end (100 bp read length), generating at least 30 M clean reads per sample on the BGI-Seq500 platform.

Data analysis and statistics

All statistics, with the exception of the RNA-seq data, were performed using GraphPad Prism software (GraphPad Software, La Jolla, CA). Data shown in graphs are from three independent experiments and represent the mean ± standard error of the mean (SEM), unless otherwise specified.

qRT-PCR analysis was done using Bio-Rad CFX Manager software. Thresholds were determined per primer pair and relative mRNA levels were calculated using the ΔΔCt method.[61] To determine the relative abundance of the different splice isoforms from the RT-PCR, the peak calling function of the QIAxcel ScreenGel software (QIAGEN) was used. The molarity of the DM1-dominant isoform (including *MBNL1* exon 5 and exon 7 or excluding *DMD* exon 78, respectively)[29,62] was divided by the sum of the molarities of all the isoforms and expressed as a percentage.

To test whether there was a difference between blocking and gapmer ASOs, a two-way ANOVA was performed with Bonferroni post tests for pairwise comparisons of repeat-targeting, non-repeat-targeting and control ASOs.

Microscopy images were analyzed using FIJI[63] (see supplemental materials and methods). In brief, slices from z stacks were combined in maximum intensity projections. Then, nuclear masks were created and nuclear foci were counted using either the "3D Objects Counter" plugin with a size filter of 15-27581040 voxels and an optimized threshold per experiment, or the "Find Maxima" function with an optimized noise tolerance per experiment. To measure MBNL1 enrichment in $(CUG)_{exp}$ foci, a mask of these nuclear RNA foci was created and MBNL1 signal was measured in each focus. The mean nuclear MBNL1 intensity in the image was subtracted from the intensity in each focus. In all cases, at least 20 nuclei were measured per condition and per independent replicate.

The change in the number of MBNL1 foci over time after ASO treatment was fitted using a sigmoidal dose-response curve, enforcing a shared value for the top of the curves. EC_{50} and bottom values were compared separately by a comparison of fits with an extra sum-of-squares F test.

Data analysis of the primary RNA-seq data was performed by BGI. Reads were filtered by internal SOAPnuke software (https://github.com/BGI-flexlab/SOAPnuke) to exclude reads that contained adapter sequences, >5% unknown bases, or >20% bases with a quality score <15. Clean reads were mapped to the Hg38 reference genome using HISAT2.[64] StringTie[65] was used to reconstruct transcripts, and novel transcripts were identified using Cuffcompare and CPC.[66,67] Novel coding transcripts were merged with reference transcripts, after which clean reads were mapped to this complete reference using Bowtie2.[68] Gene expression levels were calculated with RSEM.[69] Pearson correlation between all samples was calculated, and a hierarchical clustering analysis was performed (using the cor and hclust functions in R, respectively). Differential gene expression analysis was performed using a NOIseq algorithm.[70] Differential splicing events were detected using rMATS,[71] distinguishing five types of splicing events: skipped exon, alternative 5′ splice site, alternative 3′ splice site, mutually exclusive exons, and retained intron.

To increase the power and to correct for general non-specific effects of the ASOs, the three negative controls (untreated DM11, blocking control-treated DM11, and gapmer control-treated DM11, n = 2 each) were grouped for differential gene expression and differential splicing comparisons. In addition, three independent replicates of untreated C25 cells were included as a reference for gene expression and alternative splicing in unaffected cells.

To investigate off-target effects on other $(CUG)_n$-containing transcripts, a list of genes with ≥ 5 CTG repeats was compiled based on (1) a BLAST search of increasing lengths of $(CTG)_n$ sequences, starting from $(CTG)_5$, and (2) literature reports of $(CUG)_n$-containing transcripts.[9,18] The number of CTG triplets in the DM11 cells was determined from the RNA-seq data using the Interactive Genome Viewer. Reads spanning the entire CUG triplet repeat were used to determine the repeat length. If reads from two alleles with different CUG repeat lengths were present, we calculated the mean number of triplets. The $\log_2$-fold change and probability thereof compared with the control group were retrieved, applying cutoff values for significance of $|\log_2\text{-fold change}| \geq 1$ and probability ≥ 0.8. The same approach was used to determine effects of the ASOs on genes in the *DMPK* locus and the main DM1-associated splice factors.

To assess effects of the ASOs on DM1-associated alternative splicing, a reference list of alternative splicing events in DM1 was made based on (1) literature reports that investigated transcriptome-wide splicing changes in patient tissues and/or cell culture[39–41] and (2) an RNA-seq dataset generated by our own group,[42] comparing DM11 myoblasts with isogenic controls from which the repeat had been excised using CRISPR-Cas9.[22] For each splicing event, the genomic coordinates were retrieved and the support for an event was defined as the number of times that a certain exon or set of exons was reported to be alternatively spliced. From the data of Batra et al.,[41] splicing events that differed between control and untreated myoblasts were counted as one. Those events that were additionally normalized by the CTG-targeting guide RNA (not different between control and CTG-treated myoblasts) were counted as having a support of two. All splicing events in genes in this reference list were retrieved, provided that $p < 0.05$ for any of the specific ASOs vs. the control group, or for C25 vs. DM11. Those events that had on average ≥ 5 counts per independent replicate in at least one of the groups (controls, ASOs or C25) were used to test for overlap in altered splicing events between conditions.

PANTHER overrepresentation tests[72] (released 2019-06-06) were performed for differentially expressed genes (PANTHER version 14.1 released 2019-03-12; Reactome version 65 released 2019-03-12). The annotation datasets "PANTHER pathways," "Reactome pathways," "PANTHER GO-Slim molecular function," "PANTHER GO-Slim biological process," and "PANTHER GO-Slim cellular component" were assessed with a Fisher's exact test and Bonferroni correction for multiple testing. ReactomePA[33] and ClusterProfiler[73] were used to visualize pathway enrichment.

DATA AVAILABILITY

RNA-seq data have been deposited in the Gene Expression Omnibus (GEO) under accession number GSE130182. To review GEO accession GSE130182, go to https://www.ncbi.nlm.nih.gov/geo/query/acc.cgi?acc=GSE130182. Enter token khwxciostlgfjib into the box. The UCSC genome browser session can be viewed at: http://genome.ucsc.edu/s/leontienvdbent/RNAseq_block_or_degrade.

SUPPLEMENTAL INFORMATION

Supplemental information can be found online at https://doi.org/10.1016/j.omtn.2023.04.010.

ACKNOWLEDGMENTS

We kindly thank Dr. D. Furling and Dr. V. Mouly for providing the immortalized and primary human myoblasts that were used in this study. We thank the other members of our departments for support. This work was supported by the Prinses Beatrix Spierfonds (grant nos. W.OR14-19 and W.OR19-07).

AUTHOR CONTRIBUTIONS

Conceptualization, R.B. and D.G.W.; investigation, N.E.B., M.L.v.d.B., and M.W.; validation, N.E.B. and M.L.v.d.B.; writing – original draft, N.E.B. and M.L.v.d.B.; writing – review & editing, N.E.B., M.L.v.d.B., R.B., and D.G.W.; formal analysis, N.E.B., M.L.v.d.B., M.W., and P.A.C.'tH.; supervision, R.B. and D.G.W.

DECLARATION OF INTERESTS

D.G.W. is inventor on patents related to ASOs for treatment of myotonic dystrophy type 1.

REFERENCES

1. Uhlmann, E., and Peyman, A. (1990). Antisense oligonucleotides: a new therapeutic principle. Chem. Rev. *90*, 543–584. https://doi.org/10.1021/cr00102a001.
2. Bennett, C.F., Baker, B.F., Pham, N., Swayze, E., and Geary, R.S. (2017). Pharmacology of antisense drugs. Annu. Rev. Pharmacol. Toxicol. *57*, 81–105. https://doi.org/10.1146/annurev-pharmtox-010716-104846.
3. Aartsma-Rus, A. (2017). FDA approval of nusinersen for spinal muscular atrophy makes 2016 the year of splice modulating oligonucleotides. Nucleic Acid Therapeut. *27*, 67–69. https://doi.org/10.1089/nat.2017.0665.
4. Monia, B.P., Lesnik, E.A., Gonzalez, C., Lima, W.F., McGee, D., Guinosso, C.J., Kawasaki, A.M., Cook, P.D., and Freier, S.M. (1993). Evaluation of 2'-modified oligonucleotides containing 2'-deoxy gaps as antisense inhibitors of gene expression. J. Biol. Chem. *268*, 14514–14522.
5. Crooke, S.T., Lemonidis, K.M., Neilson, L., Griffey, R., Lesnik, E.A., and Monia, B.P. (1995). Kinetic characteristics of Escherichia coli RNase H1: cleavage of various antisense oligonucleotide-RNA duplexes. Biochem. J. *312* (Pt 2), 599–608.
6. Depienne, C., and Mandel, J.L. (2021). 30 years of repeat expansion disorders: what have we learned and what are the remaining challenges? Am. J. Hum. Genet. *108*, 764–785. https://doi.org/10.1016/j.ajhg.2021.03.011.
7. van der Bent, M.L., van Cruchten, R.T.P., and Wansink, D.G. (2019). CHAPTER 7 targeting toxic repeats. In Advances in Nucleic Acid Therapeutics (The Royal Society of Chemistry), pp. 126–150. https://doi.org/10.1039/9781788015714-00126.
8. Mulders, S.A.M., van Engelen, B.G.M., Wieringa, B., and Wansink, D.G. (2010). Molecular therapy in myotonic dystrophy: focus on RNA gain-of-function. Hum. Mol. Genet. *19*, R90–R97. https://doi.org/10.1093/hmg/ddq161.
9. Mulders, S.A.M., van den Broek, W.J.A.A., Wheeler, T.M., Croes, H.J.E., van Kuik-Romeijn, P., de Kimpe, S.J., Furling, D., Platenburg, G.J., Gourdon, G., Thornton, C.A., et al. (2009). Triplet-repeat oligonucleotide-mediated reversal of RNA toxicity in myotonic dystrophy. Proc. Natl. Acad. Sci. USA *106*, 13915–13920. https://doi.org/10.1073/pnas.0905780106.
10. Wheeler, T.M., Sobczak, K., Lueck, J.D., Osborne, R.J., Lin, X., Dirksen, R.T., and Thornton, C.A. (2009). Reversal of RNA dominance by displacement of protein sequestered on triplet repeat RNA. Science *325*, 336–339. https://doi.org/10.1126/science.1173110.
11. González-Barriga, A., Mulders, S.A., van de Giessen, J., Hooijer, J.D., Bijl, S., van Kessel, I.D., van Beers, J., van Deutekom, J.C., Fransen, J.A., Wieringa, B., and Wansink, D.G. (2013). Design and analysis of effects of triplet repeat oligonucleotides in cell models for myotonic dystrophy. Mol. Ther. Nucleic Acids *2*, e81. https://doi.org/10.1038/mtna.2013.9.
12. Leger, A.J., Mosquea, L.M., Clayton, N.P., Wu, I.H., Weeden, T., Nelson, C.A., Phillips, L., Roberts, E., Piepenhagen, P.A., Cheng, S.H., and Wentworth, B.M. (2013). Systemic delivery of a peptide-linked morpholino oligonucleotide neutralizes mutant RNA toxicity in a mouse model of myotonic dystrophy. Nucleic Acid Therapeut. *23*, 109–117. https://doi.org/10.1089/nat.2012.0404.
13. Wojtkowiak-Szlachcic, A., Taylor, K., Stepniak-Konieczna, E., Sznajder, L.J., Mykowska, A., Sroka, J., Thornton, C.A., and Sobczak, K. (2015). Short antisense-locked nucleic acids (all-LNAs) correct alternative splicing abnormalities in myotonic dystrophy. Nucleic Acids Res. *43*, 3318–3331. https://doi.org/10.1093/nar/gkv163.
14. Lee, J.E., Bennett, C.F., and Cooper, T.A. (2012). RNase H-mediated degradation of toxic RNA in myotonic dystrophy type 1. Proc. Natl. Acad. Sci. USA *109*, 4221–4226. https://doi.org/10.1073/pnas.1117019109.
15. Wheeler, T.M., Leger, A.J., Pandey, S.K., MacLeod, A.R., Nakamori, M., Cheng, S.H., Wentworth, B.M., Bennett, C.F., and Thornton, C.A. (2012). Targeting nuclear RNA for in vivo correction of myotonic dystrophy. Nature *488*, 111–115. https://doi.org/10.1038/nature11362.

16. Pandey, S.K., Wheeler, T.M., Justice, S.L., Kim, A., Younis, H.S., Gattis, D., Jauvin, D., Puymirat, J., Swayze, E.E., Freier, S.M., et al. (2015). Identification and characterization of modified antisense oligonucleotides targeting DMPK in mice and nonhuman primates for the treatment of myotonic dystrophy type 1. J. Pharmacol. Exp. Therapeut. *355*, 329–340. https://doi.org/10.1124/jpet.115.226969.

17. Jauvin, D., Chrétien, J., Pandey, S.K., Martineau, L., Revillod, L., Bassez, G., Lachon, A., MacLeod, A.R., Gourdon, G., Wheeler, T.M., et al. (2017). Targeting DMPK with antisense oligonucleotide improves muscle strength in myotonic dystrophy type 1 mice. Mol. Ther. Nucleic Acids *7*, 465–474. https://doi.org/10.1016/j.omtn.2017.05.007.

18. Jasinska, A., Michlewski, G., de Mezer, M., Sobczak, K., Kozlowski, P., Napierala, M., and Krzyzosiak, W.J. (2003). Structures of trinucleotide repeats in human transcripts and their functional implications. Nucleic Acids Res. *31*, 5463–5468. https://doi.org/10.1093/nar/gkg767.

19. Ezzat, K., Andaloussi, S.E.L., Zaghloul, E.M., Lehto, T., Lindberg, S., Moreno, P.M.D., Viola, J.R., Magdy, T., Abdo, R., Guterstam, P., et al. (2011). PepFect 14, a novel cell-penetrating peptide for oligonucleotide delivery in solution and as solid formulation. Nucleic Acids Res. *39*, 5284–5298. https://doi.org/10.1093/nar/gkr072.

20. van der Bent, M.L., Paulino da Silva Filho, O., Willemse, M., Hällbrink, M., Wansink, D.G., and Brock, R. (2019). The nuclear concentration required for antisense oligonucleotide activity in myotonic dystrophy cells. Faseb. J. *33*, 11314–11325. https://doi.org/10.1096/fj.201900263R.

21. Pettersson, O.J., Aagaard, L., Jensen, T.G., and Damgaard, C.K. (2015). Molecular mechanisms in DM1 — a focus on foci. Nucleic Acids Res. *43*, 2433–2441. https://doi.org/10.1093/nar/gkv029.

22. van Agtmaal, E.L., André, L.M., Willemse, M., Cumming, S.A., van Kessel, I.D.G., van den Broek, W.J.A.A., Gourdon, G., Furling, D., Mouly, V., Monckton, D.G., et al. (2017). CRISPR/Cas9-induced (CTG•CAG)n repeat instability in the myotonic dystrophy type 1 locus: implications for therapeutic genome editing. Mol. Ther. *25*, 24–43. https://doi.org/10.1016/j.ymthe.2016.10.014.

23. Klein, A.F., Varela, M.A., Arandel, L., Holland, A., Naouar, N., Arzumanov, A., Seoane, D., Revillod, L., Bassez, G., Ferry, A., et al. (2019). Peptide-conjugated oligonucleotides evoke long-lasting myotonic dystrophy correction in patient-derived cells and mice. J. Clin. Invest. *129*, 4739–4744. https://doi.org/10.1172/JCI128205.

24. Arandel, L., Polay Espinoza, M., Matloka, M., Bazinet, A., De Dea Diniz, D., Naouar, N., Rau, F., Jollet, A., Edom-Vovard, F., Mamchaoui, K., et al. (2017). Immortalized human myotonic dystrophy muscle cell lines to assess therapeutic compounds. Dis. Model. Mech. *10*, 487–497. https://doi.org/10.1242/dmm.027367.

25. Lo Scrudato, M., Poulard, K., Sourd, C., Tomé, S., Klein, A.F., Corre, G., Huguet, A., Furling, D., Gourdon, G., and Buj-Bello, A. (2019). Genome editing of expanded CTG repeats within the human DMPK gene reduces nuclear RNA foci in the muscle of DM1 mice. Mol. Ther. *27*, 1372–1388. https://doi.org/10.1016/j.ymthe.2019.05.021.

26. Gudde, A.E.E.G., González-Barriga, A., van den Broek, W.J.A.A., Wieringa, B., and Wansink, D.G. (2016). A low absolute number of expanded transcripts is involved in myotonic dystrophy type 1 manifestation in muscle. Hum. Mol. Genet. *25*, 1648–1662. https://doi.org/10.1093/hmg/ddw042.

27. Liu, J., Hu, J., Ludlow, A.T., Pham, J.T., Shay, J.W., Rothstein, J.D., and Corey, D.R. (2017). c9orf72 disease-related foci are each composed of one mutant expanded repeat RNA. Cell Chem. Biol. *24*, 141–148. https://doi.org/10.1016/j.chembiol.2016.12.018.

28. Gates, D.P., Coonrod, L.A., and Berglund, J.A. (2011). Autoregulated splicing of muscleblind-like 1 (MBNL1) pre-mRNA. J. Biol. Chem. *286*, 34224–34233. https://doi.org/10.1074/jbc.M111.236547.

29. Rau, F., Lainé, J., Ramanoudjame, L., Ferry, A., Arandel, L., Delalande, O., Jollet, A., Dingli, F., Lee, K.Y., Peccate, C., et al. (2015;6(May). Abnormal splicing switch of DMD's penultimate exon compromises muscle fibre maintenance in myotonic dystrophy. Nat. Commun. *6*, 7205. https://doi.org/10.1038/ncomms8205.

30. Miller, J.W., Urbinati, C.R., Teng-Umnuay, P., Stenberg, M.G., Byrne, B.J., Thornton, C.A., and Swanson, M.S. (2000). Recruitment of human muscleblind proteins to (CUG)n expansions associated with myotonic dystrophy. EMBO J. *19*, 4439–4448. https://doi.org/10.1093/emboj/19.17.4439.

31. Paul, S., Dansithong, W., Jog, S.P., Holt, I., Mittal, S., Brook, J.D., Morris, G.E., Comai, L., and Reddy, S. (2011). Expanded CUG repeats dysregulate RNA splicing by altering the stoichiometry of the muscleblind 1 complex. J. Biol. Chem. *286*, 38427–38438. https://doi.org/10.1074/jbc.M111.255224.

32. Goodwin, M., Mohan, A., Batra, R., Lee, K.Y., Charizanis, K., Fernández Gómez, F.J., Eddarkaoui, S., Sergeant, N., Buée, L., Kimura, T., et al. (2015). MBNL sequestration by toxic RNAs and RNA misprocessing in the myotonic dystrophy brain. Cell Rep. *12*, 1159–1168. https://doi.org/10.1016/j.celrep.2015.07.029.

33. Yu, G., and He, Q.-Y. (2016). ReactomePA: an R/Bioconductor package for reactome pathway analysis and visualization. Mol. Biosyst. *12*, 477–479. https://doi.org/10.1039/C5MB00663E.

34. Wang, E.T., Ward, A.J., Cherone, J.M., Giudice, J., Wang, T.T., Treacy, D.J., Lambert, N.J., Freese, P., Saxena, T., Cooper, T.A., and Burge, C.B. (2015). Antagonistic regulation of mRNA expression and splicing by CELF and MBNL proteins. Genome Res. *25*, 858–871. https://doi.org/10.1101/gr.184390.114.

35. Konieczny, P., Stepniak-Konieczna, E., and Sobczak, K. (2018). MBNL expression in autoregulatory feedback loops. RNA Biol. *15*, 1–8. https://doi.org/10.1080/15476286.2017.1384119.

36. Krafchak, C.M., Pawar, H., Moroi, S.E., Sugar, A., Lichter, P.R., Mackey, D.A., Mian, S., Nairus, T., Elner, V., Schteingart, M.T., et al. (2005). Mutations in TCF8 cause posterior polymorphous corneal dystrophy and ectopic expression of COL4A3 by corneal endothelial cells. Am. J. Hum. Genet. *77*, 694–708. https://doi.org/10.1086/497348.

37. Riazuddin, S.A., Zaghloul, N.A., Al-Saif, A., Davey, L., Diplas, B.H., Meadows, D.N., Eghrari, A.O., Minear, M.A., Li, Y.J., Klintworth, G.K., et al. (2010). Missense mutations in TCF8 cause late-onset Fuchs corneal dystrophy and interact with FCD4 on chromosome 9p. Am. J. Hum. Genet. *86*, 45–53. https://doi.org/10.1016/j.ajhg.2009.12.001.

38. Wieben, E.D., Aleff, R.A., Tosakulwong, N., Butz, M.L., Highsmith, W.E., Edwards, A.O., and Baratz, K.H. (2012). A common trinucleotide repeat expansion within the transcription factor 4 (TCF4, E2-2) gene predicts Fuchs corneal dystrophy. A. Lewin, ed. *7*, e49083. https://doi.org/10.1371/journal.pone.0049083.

39. Nakamori, M., Sobczak, K., Puwanant, A., Welle, S., Eichinger, K., Pandya, S., Dekdebrun, J., Heatwole, C.R., McDermott, M.P., Chen, T., et al. (2013). Splicing biomarkers of disease severity in myotonic dystrophy. Ann. Neurol. *74*, 862–872. https://doi.org/10.1002/ana.23992.

40. Klinck, R., Fourrier, A., Thibault, P., Toutant, J., Durand, M., Lapointe, E., Caillet-Boudin, M.L., Sergeant, N., Gourdon, G., Meola, G., et al. (2014). RBFOX1 cooperates with MBNL1 to control splicing in muscle, including events altered in myotonic dystrophy type 1. PLoS One *9*, e107324. https://doi.org/10.1371/journal.pone.0107324.

41. Batra, R., Nelles, D.A., Pirie, E., Blue, S.M., Marina, R.J., Wang, H., Chaim, I.A., Thomas, J.D., Zhang, N., Nguyen, V., et al. (2017). Elimination of toxic microsatellite repeat expansion RNA by RNA-targeting Cas9. Cell *170*, 899–912.e10. https://doi.org/10.1016/j.cell.2017.07.010.

42. André, L.M., van Cruchten, R.T.P., Willemse, M., Bezstarosti, K., Demmers, J.A.A., van Agtmaal, E.L., Wansink, D.G., and Wieringa, B. (2019). Recovery in the myogenic program of congenital myotonic dystrophy myoblasts after excision of the expanded (CTG)n repeat. Int. J. Mol. Sci. *20*, 5685. https://doi.org/10.3390/ijms20225685.

43. Yanovsky-Dagan, S., Bnaya, E., Diab, M.A., Handal, T., Zahdeh, F., van den Broek, W.J., Epsztejn-Litman, S., Wansink, D.G., and Eiges, R. (2019). Deletion of the CTG expansion in myotonic dystrophy type 1 reverses DMPK aberrant methylation in human embryonic stem cells but not affected myoblasts. Preprint at bioRxiv. https://doi.org/10.1101/631457.

44. Evers, M.M., Toonen, L.J.A., and van Roon-Mom, W.M.C. (2015). Antisense oligonucleotides in therapy for neurodegenerative disorders. Adv. Drug Deliv. Rev. *87*, 90–103. https://doi.org/10.1016/j.addr.2015.03.008.

45. Khorkova, O., and Wahlestedt, C. (2017). Oligonucleotide therapies for disorders of the nervous system. Nat. Biotechnol. *35*, 249–263. https://doi.org/10.1038/nbt.3784.

46. Aartsma-Rus, A., Straub, V., Hemmings, R., Haas, M., Schlosser-Weber, G., Stoyanova-Beninska, V., Mercuri, E., Muntoni, F., Sepodes, B., Vroom, E., and Balabanov, P. (2017). Development of exon skipping therapies for Duchenne muscular dystrophy: a critical review and a perspective on the outstanding issues. Nucleic Acid Therapeut. *27*, 251–259. https://doi.org/10.1089/nat.2017.0682.

47. Thornton, C.A., Wang, E., and Carrell, E.M. (2017). Myotonic dystrophy: approach to therapy. Curr. Opin. Genet. Dev. *44*, 135–140. https://doi.org/10.1016/j.gde.2017.03.007.

48. Liang, X.H., Nichols, J.G., Hsu, C.-W., Vickers, T.A., and Crooke, S.T. (2019). mRNA levels can be reduced by antisense oligonucleotides via no-go decay pathway. Nucleic Acids Res. *47*, 6900–6916. https://doi.org/10.1093/nar/gkz500.

49. Zu, T., Gibbens, B., Doty, N.S., Gomes-Pereira, M., Huguet, A., Stone, M.D., Margolis, J., Peterson, M., Markowski, T.W., Ingram, M.A.C., et al. (2011). Non-ATG-initiated translation directed by microsatellite expansions. Proc. Natl. Acad. Sci. USA *108*, 260–265. https://doi.org/10.1073/pnas.1013343108.

50. Pearson, C.E. (2011). Repeat associated non-ATG translation initiation: one DNA, two transcripts, seven reading frames, potentially nine toxic entities. PLoS Genet. *7*, 110020188. https://doi.org/10.1371/journal.pgen.1002018.

51. Rhodes, J.D., Lott, M.C., Russell, S.L., Moulton, V., Sanderson, J., Wormstone, I.M., and Broadway, D.C. (2012). Activation of the innate immune response and interferon signalling in myotonic dystrophy type 1 and type 2 cataracts. Hum. Mol. Genet. *21*, 852–862. https://doi.org/10.1093/hmg/ddr515.

52. Rizzo, M., Beffy, P., Del Carratore, R., Falleni, A., Pretini, V., D'Aurizio, R., Botta, A., Evangelista, M., Stoccoro, A., Coppedè, F., et al. (2018). Activation of the interferon type I response rather than autophagy contributes to myogenesis inhibition in congenital DM1 myoblasts. Cell Death Dis. *9*, 1071–1116. https://doi.org/10.1038/s41419-018-1080-1.

53. Sledz, C.A., Holko, M., de Veer, M.J., Silverman, R.H., and Williams, B.R.G. (2003). Activation of the interferon system by short-interfering RNAs. Nat. Cell Biol. *5*, 834–839. https://doi.org/10.1038/ncb1038.

54. Hornung, V., Guenthner-Biller, M., Bourquin, C., Ablasser, A., Schlee, M., Uematsu, S., Noronha, A., Manoharan, M., Akira, S., de Fougerolles, A., et al. (2005). Sequence-specific potent induction of IFN-α by short interfering RNA in plasmacytoid dendritic cells through TLR7. Nat. Med. *11*, 263–270. https://doi.org/10.1038/nm1191.

55. Senn, J.J., Burel, S., and Henry, S.P. (2005). Non-CpG-containing antisense 2'-Methoxyethyl oligonucleotides activate a proinflammatory response independent of Toll-like receptor 9 or myeloid differentiation factor 88. J. Pharmacol. Exp. Therapeut. *314*, 972–979. https://doi.org/10.1124/jpet.105.084004.

56. Vollmer, J., Weeratna, R.D., Jurk, M., Samulowitz, U., McCluskie, M.J., Payette, P., Davis, H.L., Schetter, C., and Krieg, A.M. (2004). Oligodeoxynucleotides lacking CpG dinucleotides mediate Toll-like receptor 9 dependent T helper type 2 biased immune stimulation. Immunology *113*, 212–223. https://doi.org/10.1111/j.1365-2567.2004.01962.x.

57. Paz, S., Hsiao, J., Cauntay, P., Soriano, A., Bai, L., Machemer, T., Xiao, X., Guo, S., Hung, G., Younis, H., et al. (2017). The distinct and cooperative roles of Toll-like receptor 9 and receptor for advanced glycation end products in modulating in vivo inflammatory responses to select CpG and non-CpG oligonucleotides. Nucleic Acid Therapeut. *27*, 272–284. https://doi.org/10.1089/nat.2017.0668.

58. Andaloussi, S.E.L., Lehto, T., Mäger, I., Rosenthal-Aizman, K., Oprea, I.I., Simonson, O.E., Sork, H., Ezzat, K., Copolovici, D.M., Kurrikoff, K., et al. (2011). Design of a peptide-based vector, PepFect6, for efficient delivery of siRNA in cell culture and systemically in vivo. Nucleic Acids Res. *39*, 3972–3987. https://doi.org/10.1093/nar/gkq1299.

59. Sicot, G., Gourdon, G., and Gomes-Pereira, M. (2011). Myotonic dystrophy, when simple repeats reveal complex pathogenic entities: new findings and future challenges. Hum. Mol. Genet. *20*, R116–R123. https://doi.org/10.1093/hmg/ddr343.

60. Pascual-Gilabert, M., Artero, R., and López-Castel, A. (2023). The myotonic dystrophy type 1 drug development pipeline: 2022 edition. Drug Discov. Today *28*, 103489. https://doi.org/10.1016/j.drudis.2023.103489.

61. Livak, K.J., and Schmittgen, T.D. (2001). Analysis of relative gene expression data using real-time quantitative PCR and the 2(-Delta Delta C(T)) Method. Methods *25*, 402–408. https://doi.org/10.1006/meth.2001.1262.

62. Botta, A., Malena, A., Tibaldi, E., Rocchi, L., Loro, E., Pena, E., Cenci, L., Ambrosi, E., Bellocchi, M.C., Pagano, M.A., et al. (2013). MBNL142 and MBNL143 gene isoforms, overexpressed in DM1-patient muscle, encode for nuclear proteins interacting with Src family kinases. Cell Death Dis. *4*, 7700. https://doi.org/10.1038/cddis.2013.291.

63. Schindelin, J., Arganda-Carreras, I., Frise, E., Kaynig, V., Longair, M., Pietzsch, T., Preibisch, S., Rueden, C., Saalfeld, S., Schmid, B., et al. (2012). Fiji: an open-source platform for biological-image analysis. Nat. Methods *9*, 676–682. https://doi.org/10.1038/nmeth.2019.

64. Kim, D., Langmead, B., and Salzberg, S.L. (2015). HISAT: a fast spliced aligner with low memory requirements. Nat. Methods *12*, 357–360. https://doi.org/10.1038/nmeth.3317.

65. Pertea, M., Pertea, G.M., Antonescu, C.M., Chang, T.-C., Mendell, J.T., and Salzberg, S.L. (2015). StringTie enables improved reconstruction of a transcriptome from RNA-seq reads. Nat. Biotechnol. *33*, 290–295. https://doi.org/10.1038/nbt.3122.

66. Trapnell, C., Roberts, A., Goff, L., Pertea, G., Kim, D., Kelley, D.R., Pimentel, H., Salzberg, S.L., Rinn, J.L., and Pachter, L. (2012). Differential gene and transcript expression analysis of RNA-seq experiments with TopHat and Cufflinks. Nat. Protoc. *7*, 562–578. https://doi.org/10.1038/nprot.2012.016.

67. Kong, L., Zhang, Y., Ye, Z.-Q., Liu, X.Q., Zhao, S.Q., Wei, L., and Gao, G. (2007). CPC: assess the protein-coding potential of transcripts using sequence features and support vector machine. Nucleic Acids Res. *35*, W345–W349. https://doi.org/10.1093/nar/gkm391.

68. Langmead, B., and Salzberg, S.L. (2012). Fast gapped-read alignment with Bowtie 2. Nat. Methods *9*, 357–359. https://doi.org/10.1038/nmeth.1923.

69. Li, B., and Dewey, C.N. (2011). RSEM: accurate transcript quantification from RNA-Seq data with or without a reference genome. Y. Liu, ed. *12*, 323. https://doi.org/10.1186/1471-2105-12-323.

70. Tarazona, S., García-Alcalde, F., Dopazo, J., Ferrer, A., and Conesa, A. (2011). Differential expression in RNA-seq: a matter of depth. Genome Res. *21*, 2213–2223. https://doi.org/10.1101/gr.124321.111.

71. Shen, S., Park, J.W., Lu, Z.x., Lin, L., Henry, M.D., Wu, Y.N., Zhou, Q., and Xing, Y. (2014). rMATS: robust and flexible detection of differential alternative splicing from replicate RNA-Seq data. Proc. Natl. Acad. Sci. USA *111*, E5593–E5601. https://doi.org/10.1073/pnas.1419161111.

72. Mi, H., Muruganujan, A., Ebert, D., Huang, X., and Thomas, P.D. (2019). PANTHER version 14: more genomes, a new PANTHER GO-slim and improvements in enrichment analysis tools. Nucleic Acids Res. *47*, D419–D426. https://doi.org/10.1093/nar/gky1038.

73. Yu, G., Wang, L.-G., Han, Y., and He, Q.-Y. (2012). clusterProfiler: an R Package for comparing biological themes among gene clusters. OMICS A J. Integr. Biol. *16*, 284–287. https://doi.org/10.1089/omi.2011.0118.